Hydrol. Earth Syst. Sci. Discuss., https://doi.org/10.5194/hess-2019-35
Manuscript under review for journal Hydrol. Earth Syst. Sci.
Discussion started: 4 February 2019

Hydrology and Earth System Sciences
Discussions

Hydrodynamic simulation of the effects of in-channel large woody debris on the flood hydrographs of a low mountain range creek, Ore Mountains, Germany

Daniel Rasche[1,2], Christian Reinhardt-Imjela[1], Achim Schulte[1], Robert Wenzel[1,3]

[1]Freie Universität Berlin, Department of Earth Sciences, Institute of Geographical Sciences, Berlin, 12249, Germany
[2]GFZ German Research Centre for Geosciences, Section Hydrology, Potsdam, 14473, Germany
[3]LfU State Office of the Environment Brandenburg, Potsdam, 14476, Germany

Correspondence to: Christian Reinhardt-Imjela (christian.reinhardt-imjela@fu-berlin.de)

Abstract. Fifteen years after introducing the European Union's water framework directive (WFD), most of the German surface water bodies are still far away from having the targeted good ecological status or potential. One reason are insufficient hydromorphological diversities such as riverbed structure including the absence of natural woody debris in the channels. The presence of large woody debris (LWD) in river channels can improve the hydromorphological and hydraulic characteristics of rivers and streams and therefore act positively on a river's ecology. On the contrary, floating LWD is a potential threat for anthropogenic goods and infrastructure during flood events. Concerning the contradiction of potential risks as well as positive ecological impacts, addressing the physical effects of large woody debris is highly important, for example to identify river sections in which large woody debris can remain or can be reintroduced.

Hydrodynamic models offer the possibility of investigating the hydraulic effects of fastened large woody debris. In such models roughness coefficients are commonly used to implement LWD, however, because of the complexity of the shape of LWD elements this approach seems to be too simple and not appropriate to simulate its diverse effects especially on flood hydrographs. Against this background a two-dimensional hydraulic model is set up for a mountain creek to simulate the hydraulic effects of LWD and to test different methods of LWD implementation.

The study area comprises a 282 m long reach of the Ullersdorfer Teichbächel, a creek in the Ore Mountains (South-eastern Germany). In previous studies, field experiments with artificially generated flood events have been performed with and without LWD in the channel. Discharge time series from the experiments allow a validation of the model outputs with field observations. Methodically, in-channel roughness coefficients are changed iteratively for retrieving the best fit between mean simulated and observed flood hydrographs with and without LWD at the downstream reach outlet. In addition, roughness values are modified at LWD positions only and, simplified discrete elements representing LWD were incorporated into the calculation mesh.

In general, the model results reveal a good simulation of the observed flood hydrographs of the field experiments without in-channel large woody debris. This indicates the applicability of the model used in the studied reach of a creek in low mountain

ranges. The best fit of simulation and mean observed hydrograph with in-channel LWD can be obtained when increasing in-channel roughness through decreasing Strickler coefficients by 30 % in the entire reach or 55 % at LWD positions only. However, the increase of roughness in the entire reach shows a better simulation of the observed hydrograph, indicating that LWD elements affect sections beyond their own dimensions i.e. by forming downstream wake fields. The best fit in terms of the hydrograph's general shape can be achieved by integrating discrete elements into the calculation mesh. The emerging temporal shift between simulation and observation can be attributed to mesh impermeability and element dimensions causing too intense water retention and flow alteration. The results illustrate that the mean observed hydrograph can be satisfactorily modelled using roughness coefficients. Nevertheless, discrete elements result in a better fitting shape of the simulated hydrograph.

In conclusion, a time-consuming and work-intensive mesh manipulation is suitable for analysing detailed flow conditions using computational fluid dynamics (CFD) on small spatio-temporal scale. Here, a close-to-nature design of discrete LWD objects is essential to retrieve accurate results. In contrast, the reach-wise adjustment of in-channel roughness coefficients is useful in larger scale model applications such as 1D-hydrodynamic or rainfall-runoff simulations on catchment scale.

1 Introduction

The introduction of the European Union's Water Framework Directive (WFD) in 2000 led to a reorganisation of water policy and management in the member states of the European Union (Bosenius and Holzwarth, 2006). New aims of a good ecological and chemical status were set for managing surface water bodies and groundwater (Korn et al., 2005). In Germany, only 8.2 % of the inland surface waters had reached the targeted good ecological status by the end of March 2016, while the majority of 89.1 % still fails to achieve this aim (UBA/BMUB, 2016). The main reasons for not reaching the good ecological status are agricultural nutrient immissions and in particular, the lack of hydromorphological diversity of most watercourses (UBA/BMUB, 2016).

A natural structural element of rivers and streams with forested catchments is large woody debris (LWD) (Gurnell et al., 2002; Roni et al., 2015). It is part of the permanently produced amount of plantal detritus in terrestrial ecosystems before it enters rivers and surrounding riparian areas (Wohl, 2015). In fluvial systems, large woody debris can be defined as dead organic matter with woody texture, having diameters of at least 10 cm (Kail and Gerhard, 2003). Unlike in the definition of Kail and Gerhard (2003), several studies include the length of large wood debris of at least 1 m for distinction (i.e. Gurnell et al., 2002; Andreoli et al., 2007; Comiti et al., 2008; Bocchiola, 2011; Kramer and Wohl, 2017; Wohl, 2017) and is adapted in the present study.

Large woody debris improves the physical structure of watercourses as it increases streambed heterogeneity by forming scour pools (Abbe and Montogomery, 1996), causing sediment sorting and altering water depth as well as flow velocity (Pilotto et al., 2014). Hence, the presence of large woody debris can lead to increased habitat availability in rivers and streams (Wohl,

2017). Positive ecological impacts of LWD on fish species (i.e. Kail et al., 2007; Roni et al., 2015) and the macro-invertebrate fauna (i.e. Seidel and Mutz, 2012; Pilotto et al., 2014; Roni et al., 2015) are documented.

Therefore, in stream restoration projects, the presence of large woody debris can result in rapid hydromorphological improvements (Kail et al., 2007). Consequently, wood placements have a high potential for stream restoration measures in the scope of the WFD in Germany (Kail and Hering 2005), which in turn may also function positively for the implementation of several other legal regulations on European level such as the EU's floods and habitats directive (Pander and Geist, 2013).

On the contrary, in case of drifting large woody debris during floods, elements may jam at bridges or other infrastructure and cause increased water levels, damage or completely destroy anthropogenic goods and structures (Schmocker and Hager, 2011). For this reason, LWD is removed from European rivers and streams for more than a century (Wohl, 2015) also to ensure navigability (Young, 1991) and water conveyance (Wenzel et al., 2014). As a result, the usage of LWD in river restoration in the form of leaving naturally transported woody debris in-stream or artificial wood placements is discussed controversially (Roni et al., 2015; Wohl, 2017).

With respect to the potential risks of large woody debris for anthropogenic goods on the one hand and high ecological benefits on the other, it may be necessary to distinguish river sections in which large wood can remain or be introduced from those where it needs to be removed (Wohl, 2017). Large wood related segmentation of rivers and streams requires knowledge of the physical effects caused by mobile and stable in-channel large woody debris. Although several studies investigate the general hydraulic impact of LWD in field studies (i.e. Daniels and Rhoads, 2004; Daniels and Rhoads, 2007; Wenzel et al., 2014) and laboratory experiments (i.e. Young, 1991; Davidson and Eaton, 2013; Bennett et al., 2015) regarding the alteration of water level, flow pattern, flow velocity and discharge, a project and site specific examination is necessary to evaluate local consequences of intended stream restoration measures.

The resulting physical effects of stable in-channel LWD can be addressed using hydrodynamic models (Smith et al., 2011). Several studies consider large woody debris in the scope of one- and two-dimensional hydrodynamic simulations for example for investigating its influence on flood hydrographs (Thomas and Nisbet, 2012), on floodplain connectivity (Keys et al., 2018) or are considered in research applications with an ecological focus (i.e. He et al., 2009; Hafs et al., 2014; Lange et al., 2015). Furthermore, representing and integrating of large woody debris elements in hydrodynamic models is addressed in different studies using three-dimensional hydrodynamic models (i.e. Smith et al., 2011; Allen and Smith, 2012; Lai and Bandrowski, 2014; Xu and Liu, 2017).

Despite the necessity of a discrete representation of large woody debris elements in the calculation mesh of hydrodynamic models for obtaining accurate results, LWD elements are often accounted for using roughness coefficients in hydrodynamic model applications (Smith et al., 2011). The impact of large woody debris on in-channel roughness is investigated by Gregory et al. (1985), Shields and Smith (1992), Shields and Gippel (1995), Dudley et al. (1998), MacFarlane and Wohl, (2003) and Wilcox and Wohl (2006). In addition, Curran and Wohl (2003) and Wilcox et al. (2006) have studied its partial contribution to channel roughness coefficients. However, a methodological lack remains in quantitatively estimating LWD related changes of in-channel roughness coefficients (Wohl, 2017), especially under field conditions (Wilcox et al., 2006).

Against this background, the aim of the present study is to quantify the influence of LWD elements on in-channel roughness coefficients in a creek in low mountain ranges using a two-dimensional hydrodynamic model and previously conducted field experiments, explicitly described in Wenzel et al. (2014). The field data offer the opportunity to validate simulated large wood related hydraulic effects on hydrographs of small flood events. In addition, different methods of implementing stable LWD are examined and evaluated, for example by altering reach-wise in-channel roughness coefficients on the one hand or as discrete roughness elements in the calculation mesh on the other.

By investigating the effects of stable LWD on reach-wise roughness coefficients and possibilities to represent LWD elements in hydrodynamic models, the present study will contribute to the understanding of the hydraulic impact of large woody debris in fluvial environments as well as its simulation and prediction. Understanding its effects and the ability of predicting hydraulic impacts of LWD in hydrodynamic simulations can be highly important for the use of LWD in stream restoration projects and ecological-orientated management approaches in the scope of the WFD.

2 Study area

The study area comprises a 282 m long section of the Ullersdorfer Teichbächel, a small first order headwater creek located in the Ore Mountains, south-eastern Germany. The catchment of the Ullersdorfer Teichbächel covers an area of 1.8 km² and drains into the river Elbe via several higher order tributaries including Schwarze Pockau, Flöha, Zschopau and Mulde.

The study reach is located in the catchment's centre and approximately 50 m downstream of an artificial rafting pond built in the 16th century. Two Thomson-weirs mark the study reach's upper and lower limits at elevations of 754.1 and 744.5 a.s.l. (Fig. 1) resulting in a difference in elevation of 10.4 m and an average channel gradient of 3.7 %. Channel dimensions vary strongly along the study reach i.e. channel width ranges from 0.8 to 0.3 m (Wenzel et al., 2014). Similarly, a high variability of stream bed grain sizes can be detected. Moderately steep sections with a sand and fine gravel dominated bed structure alternate with reach sections of higher gradients dominated by coarse gravel, cobbles and small boulders with sizes of up to 0.3 m in diameter. The boulders consist of gneiss varieties representing the dominating bed rock formations in the catchment. Beside a highly variable stream width, alternating slope gradients and grain sizes lead to a highly diverse distribution of stream depth along the study reach and hence, a generally complex channel structure.

The overall morphological character along the 282 m study reach consists of riffle-pool sequences in moderately steep sections as well as step-pool morphologies along sections having smaller channel widths and larger in-channel boulders. In the latter, channel-spanning steps with corresponding hydraulic jumps and eroded pools have been observed in May 2017.

The majority of the catchment of the Ullersdorfer Teichbächel is covered with coniferous forest on largely cambisols and podzols including scattered deciduous trees sprinkled in. The dominating species is spruce (*Picea abies*) with occasional occurrence of mountain pines (*Pinus mugo*) and beech trees (*Fagus sylvatica*) (Wenzel et al., 2014). Trees occur only scatteredly in the narrow floodplain along the channel of the study reach with grassy vegetation on fluvic gleysols covering most parts. However, smaller floodplain sections are covered with bare soil or leaf litter. Perpendicular to the direction of flow,

the maximum width of the floodplain measured from channel banks varies between 7 and 0 m, when channel banks immediately change into the embankments confining the study reach in length.

At the nearest gauging station Zöblitz, which is located approximately 13 km downstream the catchment's outlet at the river Schwarze Pockau and drains an area of 125 km², the mean annual discharge is 2.29 $m^3 s^{-1}$. If the value is extrapolated using a regional analyses based on drainage areas the mean discharge at the outlet of the study reach is 16 $l s^{-1}$. The flow regime of the study area is dominated by snow melt generating high flows in March and April (gauge Zöblitz, period 1937 to 2015; LfULG, 2017a). Floods of low to medium magnitudes are generated by intense snowmelt and rainfall on snow in spring or by storm events in summer. Larger flood events are caused by summer storms only (Petrow et al., 2007) but the flood magnitudes are strongly influenced by land use and are greatly affected by past forest changes (Reinhardt-Imjela et al., 2018).

3. Methods

3.1 The hydrodynamic model HYDRO_AS-2D

In this study, the two-dimensional hydrodynamic model HYDRO_AS-2D (version 2.2) is used to simulate the flow in the study reach with and without LWD. HYDRO_AS-2D was developed for practical applications in water management (Nujić, 2006) and is used in several studies simulating flow conditions in river sections (i.e. Lange et al. 2015) as well as in flood risk management applications. Especially in southern Germany and Austria, HYDRO_AS-2D became a standard 2D modelling system for hydrodynamic model applications (Faber et al., 2012). Due to the numerical approaches used in the modelling system, HYDRO_AS-2D is capable of accurately simulating mass exchange between channel and forelands, streams comprising hydraulic jumps, steep channel sections as well as high variability of channel width (Nujić, 2006).

HYDRO_AS-2D solves the two-dimensional shallow water equations (SWC) at each node of a linear calculation mesh composed of quadrilateral and triangular elements of different sizes, representing a digital terrain model of the channel and the forelands. Shallow water equations are solved using finite volume approximations for spatial discretion, while time is discretized using second order Runge-Kutta methods (Nujić, 2006). Water flow is computed through all sides of the control volume around each node using different order polynomials and upwind schemes (Nujić, 2006). Surface roughness is represented by Strickler coefficients defined for each element of the calculation mesh. Similarly, local viscosity can be defined for each mesh element. Mesh generation, pre-processing, the setting of model boundary conditions as well as simulation result visualisation of HYDRO_AS-2D v2.2 is conducted using the software Surface Water Modelling System (SMS) v10.1 (Aquaveo Inc., USA).

3.2 Datasets and mesh generation

The presented study is based on data previously collected during field experiments in March 2008 (Wenzel et al. 2014) in the river section under investigation. In this earlier study, the pond upstream the experimental reach was dammed using a flap gate weir and multiple flood waves of equal magnitude (return period of 3.5 years) were generated. The first 8 experimental runs

were conducted with 9 large woody debris elements (spruce tree tops with a length ranging from 3 to 11.5 m, mean length 8.5 m), which were placed and fastened in the channel lengthwise 9 months earlier. After the experimental runs with LWD, all LWD elements were removed and 12 additional flood waves were generated without the trees. During all experimental runs, water levels were continuously recorded with a temporal resolution of 1 s at the beginning and end of the river section using Thomson-weirs equipped with pressure gauges. For each Thomson-weir, the averaged (mean) hydrograph of experimental runs with and without LWD is calculated and used as the upper model boundary condition (Thomson-weir 1) and for the validation of model outputs (lower boundary condition, Thomson-weir 2), respectively.

During the development of the hydraulic model, a measurement error was detected in the water level measurement at Thomson-weir 1 (input weir), which results in a significantly lower discharge volume at Thomson-weir 2, although larger water inflows between both weirs were not observed in the field. The measurement error of the input weir was corrected by increasing water levels in the original water level time series of the pressure gauge and recalculating discharge. The measured water levels at the first weir had to be increased by a maximum of 2.4 cm until the total flood volume at both weirs was nearly equal.

To generate a digital terrain model (DTM) for the studied river section, data from a cross-sectional geodetic survey conducted with Spectra Precision AB Geodimeter 400 in 2008 were available. To improve the implementation of the channel in the hydrodynamic model the channel width was surveyed again in intervals of 5 m using a measuring stick in May 2017. Furthermore, a digital elevation model with a spatial resolution of 2 x 2 m (Saxon State Office of Geoinformation and Surveying, 2008) is used for better reproduction of the floodplain morphology. The final DTM for the model is generated from processing and combining all topographic datasets in the software environment ArcGIS v10.5 (ESRI Inc., USA). The resulting DTM is exported as equally spaced elevation points with a spatial resolution of approximately 0.5 x 0.5 m for the entire study reach including riparian areas and embankments. From the point grid the calculation mesh required for simulations with HYDRO_AS-2D is created. Mesh generation is done in the software environment SMS v10.1 and according to mesh quality requirements of HYDRO_AS-2D, such as minimum and maximum angle of mesh elements or maximum number of element connections per node (Nujić, 2006). The calculation mesh is composed of quadrilateral and triangular elements. In the channel of the study reach, quadrilateral elements are created by stepwise mesh generation between cross-sectional point elevation profiles through linear interpolation of elevation between profiles. A triangular mesh is generated in the riparian areas and along embankments by using equally spaced elevation points. After merging quadrilateral channel elements and triangular foreland elements as well as including additional topographic features to the calculation mesh (fig. 3) to match field observations, roughness coefficients are assigned to each mesh element. The Strickler coefficients k_{st} were estimated during field surveys in May 2017 with reference to established roughness coefficient classifications for different land cover and surface material types (i.e. Chow, 1959) as well as in accordance with observed ground cover during field experiments in 2008.

3.3 Hydrodynamic modelling

Boundary conditions for the unsteady hydrodynamic simulations are defined in SMS v10.1. For flow simulations of the experimental reach without LWD, the averaged discharge time series without LWD at Thomson-weir 1 (Fig. 2) is defined as

the water inflow into the study reach. Water influx is defined at the location of Thomson-weir 1 in the calculation mesh, represented by the uppermost cross-sectional nodestring in the channel. For the simulations with in-channel LWD, the averaged time series with LWD at Thomson-weir 1 (Fig. 2) is used as the system input.

For the simulations without and with LWD, the inflow hydrographs at Thomson-weir 1 are extended forwardly by 5400 seconds using the first discharge value of the corrected mean experimental hydrograph without and with LWD. This is done to achieve field conditions of minor flow through the channel in the study reach before the experimental flood waves enter the channel. This results in a total simulation time of 9000 seconds for each simulation with and without LWD with a temporal resolution of 1 second.

Simulation results are obtained at the location of Thomson-weir 2 in the calculation mesh represented by the lowermost cross-sectional nodestring in the channel of the study reach. Model performance is assessed by visual comparison of mean observed and simulated flood hydrographs without and with LWD at Thomson-weir 2 as well as by calculating the statistical goodness of fit parameters Nash-Sutcliff-Efficiency (NSE), percent bias (PBIAS) and RSR (ratio of the root mean square error to the standard deviation of observed values) using the hydroGOF package by Zambrano-Bigiarini (2017) in R (R Core Team, 2017).

3.4 Hydrodynamic simulation variants

In the scope of this study, four different simulation variants are applied to investigate effects of in-channel large woody debris on flood hydrographs in a small low mountain stream: (1) the base variant BV representing the simulation of field experiments without in-channel LWD and (2-4) variants V1 to V3 for simulating field experiments with LWD.

Variant BV is used to obtain the best fit of the mean observed and simulated hydrograph without LWD at Thomson-weir 2 through iteratively adjusting Strickler roughness coefficients in the channel and in riparian areas. In the base variant and all simulation variants calibration is performed to achieve the best possible simulation of the moment of rise, the rising limb and peak discharge of the mean observed hydrograph at Thomson-weir 2. Calibrated roughness coefficients leading to the best fit in variant BV will be used as initial roughness coefficients in the calculation mesh of variants V1, V2 and V3.

Variant V1 represents the first simulation with LWD. Calibrated Strickler coefficients from variant BV are iteratively adjusted for the entire channel (integrated roughness). Adjustments are made percent-wise and with equal magnitude to enable equal scaling of spatially varying roughness coefficients of mesh elements in the channel. This approach was included because the integrated channel roughness of a river section is an important input parameter for rainfall-runoff models at mesoscale or of larger watersheds, which often use only one Strickler (or Manning) coefficient per section.

Similarly, roughness is scaled in **variant V2**, in which Strickler coefficients from variant BV are adjusted at the positions of all LWD elements only. LWD element locations and corresponding LWD influenced channel sections (length of each LWD element) are derived from Wenzel et al. (2014). For each channel section roughness coefficients are adjusted percent-wise and with equal magnitude.

In contrast to variants V1 and V2, where LWD is represented by reach-wise and section-wise adjustment of Strickler coefficients of quadrilateral in-channel calculation mesh elements, **variant V3** includes the integration of simplified discrete

roughness elements by manipulating the existing calculation mesh used in variant BV. Therefore, discrete elements with the maximum stem length and width (without branches) of each individual LWD are incorporated into the calculation mesh by creating corresponding rectangular polygons overlying the mesh. Polygons are positioned in order to have the largest possible part located in the channel of the study reach. Based on the existing calculation mesh, new mesh nodes are positioned in 20 cm intervals along polygon boundaries and within a 10 cm distance outside polygons. Nodes along polygon boundaries receive the elevation of the closest upstream node increased by 150 cm. The elevation of nodes within 10 cm distance are interpolated from the existing calculation mesh. As mesh quality requirements (see chapter 3.2) need to be maintained, positions of some added nodes are slightly shifted. Additional quadrilateral and triangular mesh elements are created between nodes added to the mesh. All newly created mesh elements representing discrete LWD elements (Fig. 3) are parameterized with the same Strickler coefficient in order to retrieve the best fit between simulated and mean observed hydrograph with LWD at Thomson-weir 2. Strickler coefficients of mesh elements representing discrete large woody debris elements are used to account for i.e. branches of real spruce tree tops implemented into the channel during the field experiments. Coefficients are determined iteratively during calibration of simulation variant V3.

4. Results

4.1 Simulation variant BV

In the base variant, the best fit in the unsteady hydrodynamic simulation without LWD was achieved with in-channel Strickler coefficients ranging from 6 $m^{1/3}$ s^{-1} for channel sections with larger boulders to 12 $m^{1/3}$ s^{-1} in channel sections where fine gravel forms the stream bed. A Strickler coefficient of 3.5 $m^{1/3}$ s^{-1} was defined for riparian areas during calibration.

Observed and simulated hydrographs of the simulation are shown in fig. 4. In general, the model simulates the characteristics of the observed hydrograph very well. Only the crest is slightly wider in the model and a slight model underestimation can be observed at the beginning and in the second half of the simulation time. The good model performance is reflected by a high NSE of 0.99 as well as a low RSR (0.11) and PBIAS (-3.5 %). The statistical goodness-of-fit parameters of all simulation variants are summarized in table 2. The cumulative maximum inundated area comprises 739 m², defined as the total area of mesh elements inundated during simulation.

4.2 Variant V1 - Integrated increase of roughness in the channel

In the first simulation variant V1 of field experiments with in-channel large woody debris, Strickler coefficients were decreased in the entire channel based on the coefficients of the simulation without large wood (variant BV). A decrease of Strickler values and hence, an increase of roughness of 30 % in the entire channel resulted in the best fit between mean observed and simulated hydrograph. Consequently, in-channel Strickler coefficients range from 4.2 to 8.4 $m^{1/3}$ s^{-1} in variant V1. The 9 LWD elements in the field investigations cover 75.1 m of the 282 m long channel reach, i.e. the simulated 30 % increase of the integrated channel roughness refers to a LWD percentage of 27 % of the channel length.

The resulting simulated hydrograph of variant V1 shows a good representation of the time of rise as well as the rising limb of the observed hydrograph (Fig. 4). However, in the peak discharge phase the simulated hydrograph does not rise continuously until peak values are reached. If the Strickler coefficients in the channel foreland (riparian area) were decreased from 3.5 to 2.4 $m^{1/3}$ s^{-1} in addition to the channel roughness, the break in the crest of the hydrograph disappears. After adjusting roughness coefficients in riparian areas, rising limb and peak phase of the observed hydrograph are represented slightly better. Nevertheless, discharge values during peak phase show a distinct underestimation of observed values. Similarly, differences can be found along the falling limb between observation and simulation. The maximum inundated area comprises 861 m² before and 880 m² after riparian roughness adjustment. Nash-Sutcliffe-Efficiency values of 0.97 before and 0.98 after adjustment of roughness coefficients in riparian areas were achieved. The RSR shows values of 0.18 and 0.14 before and after adjustment, while PBIAS slightly increases after adjustment from -3.6 to -3.7 %. (Table 2).

4.3 Variant V2 - Increase of roughness at LWD spots

In simulation variant V2, in-channel roughness coefficient derived from variant BV were altered in large woody debris affected channel spots only. Here, a reduction of Strickler coefficients of 55 % resulted in the best fit of observed and simulated hydrographs. Depending on the LWD affected channel section, Strickler coefficients between 3.6 and 5.4 $m^{1/3}$ s^{-1} were derived. The resulting simulated hydrograph properly represents the time of rise. Compared to variant V1, the rising limb is less accurately modelled. Similarly to variant V1, a discontinuous peak phase is generated in the simulations. Again, an increase of the roughness in riparian areas is necessary to simulate a hydrograph with a more realistic, continuous rise of discharge up to the crest of the hydrograph. Strickler coefficients in riparian forelands were reduced from 3.5 to 1.9 $m^{1/3}$ s^{-1}. In addition, both simulated hydrographs (with and without subsequent adjustment of riparian roughness coefficients) show an overestimation of the observed discharge along the falling limb of the flood wave, while a distinct underestimation can be observed during the peak phase as well as in the beginning and the end of the experiments (Fig. 4). Before adjusting riparian surface roughness, the maximum cumulative inundation area is 859 m². After subsequent adjustment inundated area rises to 892 m². NSE values range from 0.94 before to 0.96 after adjusting riparian Strickler coefficients, while RSR decreased from 0.24 to 0.19 and PBIAS from -4.2 to -4.0 (Table 2). With regard to the general shape of simulated hydrographs as well as the statistical model performance assessment, variant V1 reveals a better representation of the observed hydrograph of the field experiments with in-channel large woody debris.

4.4 Variant V3 - Implementation of LWD as discrete elements

In the last simulation variant (V3), large woody debris is integrated into the model as simplified discrete elements by manipulating the calculation mesh. The created mesh elements representing discrete LWD elements received a Strickler coefficient of 8.5 $m^{1/3}$ s^{-1} to account for branches and in order to obtain the best fit between mean observed and simulated hydrograph. As shown in fig. 4, the simulated hydrograph rises slightly later than the mean observed hydrograph, which results in differences between simulation and observation along the falling limb. Additionally, a slight overestimation of peak

discharges can be observed as well as the underestimation of discharges in the beginning and end of the simulation. The maximum water covered area comprises 927 m² and is much larger than in previous simulation variants. Statistical goodness-of-fit parameters show a NSE value of 0.90, a RSR value of 0.32 and PBIAS of -7.7 %. Especially the PBIAS of variant V3 is much higher than in all other simulation variants (Table 2). According to the classification of Moriasi et al. (2007), goodness-of-fit parameter values calculated for variant V3 as well as for all other simulation variants in this study indicate very good simulation results. Despite the temporal shift between the average simulated and observed flood hydrograph as well as the lower goodness-of-fit according to the classification of Moriasi et al. (2007), the general narrow shape of the flood hydrograph of the field experiments with in-channel LWD is most accurately modelled in variant V3.

5. Discussion

5.1 Simulations of flood hydrographs in the investigated creek section

In general, the 2D hydrodynamic model mimics the flow conditions of the field experiments without LWD (variant BV) very well. Especially the time of rise, the rising limb and the flood peak are well represented, minor deviations can be observed along the hydrograph's falling limb only due to the broader shape of the simulated hydrograph. However, it has to be noted that measurement errors may also occur in the field data demonstrated by the fact that the input time series measured at Thomson weir-1 had to be corrected to reduce the volume error between both weirs. After the correction, the cumulated volume error between both weirs was reduced to 4 $m^3 h^{-1}$ without LWD and 5 $m^3 h^{-1}$ for the field experiments with LWD (1 l/s) (Table 1). The remaining difference between both weirs lies in the range of what can be estimated as natural water influx between both weirs based on runoff per km² estimations from regional analyses of the nearest gauging station for the days of the field experiments (LfLUG, 2017b). Depending of the spatial resolution of the DTM used for calculation (2 and 5 m), the average water influx ranges from 3 to 6 $m^3 h^{-1}$. Hence, the remaining volumetric difference can be attributed to diffuse lateral water influx during the run time of each experiment and are likely to be responsible for the modelled (Fig. 4) and observed (Fig. 2) lower discharges before and after flood passage at Thomson-weir 2. However, after correction it can be assumed that the measured data are a reliable reference for the hydrodynamic simulation.

The broader shape of the simulated hydrograph is likely to be caused by the calculation mesh used, representing the terrain surface. The calculation mesh is based on topographic field data gathered in the scope of the field experiments in 2008 to find most suitable locations to position large woody debris elements (Wenzel et al., 2014). Therefore, small topographic features in the channel and adjacent riparian areas are not included in the elevation data set and hence, in the calculation mesh. This especially applies to step-pool sequences in the study reach. Steps and pools produce rapid flow energy losses caused by corresponding hydraulic jumps and resulting in a deceleration of flow (Wilcox et al., 2011), where the amount of energy loss dynamically depends on water level (Comiti et al., 2009). Furthermore, erosion and transport of bed material leads to flow energy losses (Yen, 2002). As such features are missing in the calculation mesh, roughness coefficients are used to account for their impact on water flow. However, calibrating in-channel roughness coefficients may lead to a much more continuous

decrease of flow velocities instead of intense, punctual flow decelerations with implications for downstream flow conditions, in turn resulting in a broader peak of the simulated flood hydrograph. This illustrates the necessity of a high resolution calculation mesh including small scale topographic features in the channel and microtopography in riparian areas to obtain accurate model results.

Despite the discrepancies described above, the simulation of variant BV shows a very precise simulation of the observed hydrograph of the field experiments without large woody debris, which is also indicated by the statistical goodness-of-fit parameters revealing a very high model accuracy according to the classification of Moriasi et al. (2007). Hence, averaged flood hydrographs of the field experiments without large woody debris can be accurately simulated using the set-up model, illustrating its applicability for simulating the flow conditions in the study reach.

5.2 Simulating the hydraulic impact of stable in-channel LWD using roughness coefficients

In simulation variants V1 and V2, roughness coefficients are used to represent large woody debris in the study reach. Both variants show a correct simulation of the time of rise of the flood hydrograph. Differences occur along the rising limb as well as the hydrograph's peak. Here, variant V1 produces a better fitting hydrograph. Compared to the simulation result of the mean observed hydrograph of the field experiments without in-channel LWD, variants V1 and V2 produce less well fitting simulated hydrographs, which is also indicated by the slightly lower values of statistical goodness-of-fit parameters. Nevertheless, these values still indicate a very high model accuracy.

For both simulation variants, subsequent adjustment of riparian roughness coefficients is necessary to improve the goodness-of-fit. Only increasing riparian roughness by decreasing Strickler coefficients results in a smooth crest as it can be originally observed in the field experiments. In the model, water flows too fast through adjacent riparian areas without subsequent adjustment of roughness. Emerged riparian vegetation can lead to an increase of Manning's n and hence, a decrease of Strickler coefficients due to increasing friction exerted on flow (Shields et al., 2017). Therefore, generally low flow depths, a largely continuous cover of dense grassy vegetation as well as a uneven microtopography due to i.e. elevated grass root wads observed in adjacent riparian areas during field experiments may have led to the necessity of increasing local roughness; especially due to the lack of such features in the model's calculation mesh.

Simulation variant V1 produces a better representation of the average observed hydrograph of field experiments with in-channel LWD by increasing roughness in the entire channel of the study reach instead of increasing roughness at LWD affected spots only (V2). In-channel LWD elements decelerate flow beyond their own dimensions by generating upstream backwater areas and downstream wake fields of substantial length (i.e. Young, 1991; Bennett et al., 2015). Such features were also observed during field experiments (Wenzel et al., 2014). That means that LWD affects flow upstream and downstream in an area which is larger than the wood piece itself, which can be one reason for the slightly better simulation results in V1 compared to V2.

Decreasing Strickler coefficients by 30 % in variant V1 compared to 55 % in LWD affected spots only (V2) are in the range of previous studies. For instance, Gregory et al. (1985) detected an LWD related increase in Manning's n by 48.5 % and Dudley

et al. (1998) show an average increase of 36 %. Furthermore, MacFarlane and Wohl (2003) compare streams with and without LWD and find Darcy-Weisbach's f on average 58 % higher in streams containing in-channel LWD. However, it should be noted that boundary conditions, such as discharge, river size, LWD volume, etc. as well as the methodological approaches greatly vary between studies, illustrating the need of a common framework for better comparability of studies on large woody debris previously proposed by Wohl et al. (2010). This becomes especially true regarding the influence of stable in-channel LWD on roughness coefficients.

5.3 Representation of in-channel LWD as discrete elements

Although roughness coefficients are often used to account for the hydraulic influence of stable in-channel large woody debris, the implementation of LWD as discrete elements in the calculation mesh may further improve simulation results (Smith et al., 2011). However, field data are an essential reference to compare the implementation of wood by altering in-channel roughness coefficients with the implementation of discrete elements in the calculation mesh.

Nevertheless, one problem of discrete LWD elements in hydrodynamic models is that wood pieces have a complex shape, which strongly varies from piece to piece (and over time) concerning their geometry with twigs, branches, needles and floating debris caught up in the twigs. This complex shape as well as a permeability of LWD elements and jams cannot be implemented in depth-averaged hydrodynamic models in detail and has to be simplified. The simplified implementation can be the reason, why variant V3 produces a temporal shift between mean simulated and observed flood hydrograph causing a slightly delayed rise and falling limb of the flood hydrograph and hence, a delayed passage of the flood wave at Thomson-weir 2. This indicates too strong flow alterations in the model resulting in higher amounts of water retained in the study reach. In this study, LWD elements are implemented as discrete parts of the calculation not allowing water flowing through. Hence, they are designed with too extensive simplifications to account for the complexity of real LWD elements.

Nevertheless, the variant V3 generates the best simulated hydrograph in regard to its overall shape compared to the mean observed hydrograph of field experiments with LWD, indicating that discrete elements are a very good starting point for an advancement of model implementation and further studies on the hydrodynamics of in-channel LWD. This is in accordance with previous studies using three-dimensional hydrodynamic models (computational fluid dynamics, CFD). On the one hand, general flow patterns caused by large wood can be simulated using impermeable discrete elements, when an accurate simulation of flow near LWD objects is neglectable (Xu and Liu, 2017). On the contrary, simplifications of LWD objects made during the integration process into the calculation mesh may cause deviations and inaccuracies (Allen and Smith, 2012). Impermeability, dimensions and positions of elements result in too strong flow alterations and a temporal shift of the modelled hydrograph, while its general shape indicates the best simulation of flow processes in the study reach. Intense flow alterations may also account for the fact that a subsequent adjustment of riparian roughness coefficients is not required in variant V3, as too strong energy losses and flow declarations caused by discrete LWD objects account for roughness originally caused by other roughness elements not represented in the calculation mesh such as riparian vegetation and microtopography.

Nevertheless, variant V3 still shows a very high goodness-of-fit. A similarly high Nash-Sutcliff-Efficiency was obtained in the study of Keys et al. (2018), who use discrete weirs to represent large woody debris objects for simulating their effects on floodplain connectivity. However, although variant V3 reveals the best simulation result, the temporal shift results in a lower goodness-of-fit and hence, model quality compared to simulation variants V1 and V2. Therefore, solely relying on statistical goodness-of-fit indicators on such high spatio-temporal scale may not be sufficient and visual interpretation should not be excluded when assessing model results.

6. Conclusion

The hydrodynamic simulations conducted in the present study show that average flood hydrographs of previously conducted field experiments without in-channel LWD can be accurately simulated in the small and high gradient study reach. Nevertheless, minor discrepancies need to be taken into account, which can be attributed to lateral water influx between both weirs as well as a calculation mesh based terrain datasets lacking of small scale topographic features such as step-pool sequences and riparian microtopography. For this reason, high resolution topographic datasets acquired with high resolution survey techniques such as terrestrial LiDAR are required to obtain most accurate model results on such high spatio-temporal scale. In addition, in the present study calibration is solely conducted using the hydrograph at Thomson-weir 2. As point measurements of flow depth, velocity and inundation extent in the field would improve model accuracy assessments, multi-criteria calibration approaches may be considered in future studies simulating the hydraulic effects of stable in-channel large wood.

The effect of stable in-channel LWD can be accurately simulated using roughness coefficients as it is often done in hydrodynamic model applications. However, differences in model quality can be detected between increasing in-channel roughness in the entire reach or in LWD affected spots only. A reach-wise decrease of Strickler coefficients and in turn, increase of Manning's n by 30 % is comparable to previous studies investing the impact of LWD on channel roughness coefficients. This reveals better simulation results than solely increasing roughness in LWD spots by 55 %, due to large woody debris elements affecting channel flow in sections beyond their own dimensions by i.e. forming downstream wake fields. Therefore, a reach-wise alteration of in-channel roughness coefficients results in the best simulation of LWD related hydraulic effects on reach scale flood hydrographs.

Most accurate simulations of LWD related impacts on flood hydrographs regarding its overall shape can be obtained using discrete large wood elements as proposed in previous studies (Smith et al. 2011). Here, a close-to-nature design of discrete elements in the calculation mesh is essential for precise model results and in order to reduce uncertainties caused by element simplification, dimensioning and positioning (Allen and Smith, 2012). A close-to-nature representation does include element or jam permeability. However, naturally occurring flow through branches, under and over large woody debris objects cannot be accounted for in depth-averaged two-dimensional hydrodynamic models. Combined with the high amount of work and time consumption required for implementing discrete elements in a calculation mesh (Lai and Bandrowski, 2014), discrete large

woody debris objects may be most applicable in detailed investigations with three-dimensional models on high spatial-temporal scales, where a detailed simulation of the resulting flow conditions is required. Discrete elements in two-dimensional hydrodynamic model applications may be used in the scope of preliminary studies where minor deviations are neglectable. In contrast, altering roughness coefficients to represent stable large woody debris is less work-intensive and time-consuming. Hence, it may be applied to represent in-channel large woody debris on a larger spatio-temporal scale such as the catchment scale using one- and two-dimensional hydrodynamic models or in rainfall-runoff simulations, where minor differences are smaller than the overall model uncertainty. As the impact of large wood on reach-wise in-channel roughness coefficients depends on several factors including channel-width, water level, slope as well as LWD size, amount, orientation and position, ensemble-simulations with literature-based values of roughness increase may be used to simulate the influence of large woody debris. Here, reviews of recent advances in research on the hydraulics of LWD in fluvial systems would be highly beneficial; similar to recent reviews and meta-analyses addressing ecological implications (i.e. Roni et al., 2015), large wood dynamics (i.e. Ruiz-Villanueva et al., 2016; Kramer and Wohl, 2017), related risks for anthropogenic infrastructure (i.e. De Cicco et al., 2018) and large wood in fluvial systems in general (Wohl, 2017).

References

Abbe, T. B. and Montgomery, D. R.: Large woody debris jams, channel hydraulics and habitat formation in large rivers, Regulated Rivers: Research & Management 12 (2-3), 201-221, https://doi.org/10.1002/(SICI)1099-1646(199603)12:2/3<201::AID-RRR390>3.0.CO;2-A, 1996.

Allen, J. B. and Smith, D. L.: Characterizing the impact of geometric simplification on large woody debris using CFD, International Journal of Hydraulic Engineering 1 (2), 1-14, https://doi.org/10.5923/j.ijhe.20120102.01, 2012.

Andreoli, A., Comiti, F., and Lenzi, M. A.: Characteristics, distribution and geomorphic role of large woody debris in a mountain stream of the Chilean Andes, Earth Surface Processes and Landforms 32 (11), 1675-1692, https://doi.org/10.1002/esp.1593, 2007.

Bennett, S. J., Ghaneeizad, S. M., Gallisdorfer, M. S., Cai, D., Atkinson, J. F., Simon, A., and Langendoen, E. J.: Flow, turbulence, and drag associated with engineered log jams in a fixed-bed experimental channel, Geomorphology 248, 172-184, https://doi.org/10.1016/j.geomorph.2015.07.046 , 2015.

BKG – German Federal Office for Cartography and Geodesy (Ed.): German administrative units ATKIS-VG2500, scale 1:2,500,000, http://www.geodatenzentrum.de/geodaten/gdz_rahmen.gdz_div?gdz_spr=deu&gdz_akt_zeile=5&gdz_anz_zeile=1&gdz_unt_zeile=19&gdz_user_id=0, last accessed on 24-02-2018, 2018.

BMUB/UBA – German Federal Ministry for Environment, Environmental Protection, Construction and Nuclear Safety/German Federal Office for the Environment (Ed.): Die Wasserrahmenrichtlinie – Deutschlands Gewässer 2015, Bonn, Dessau, 2016.

Bocchiola, D.: Hydraulic characteristics and habitat stability in presence of woody debris: A flume experiment, Advances in Water Resources 34 (10), 1304-1319, https://doi.org/10.1016/j.advwatres.2011.06.011, 2011.

Bosenius, U. and Holzwarth, F.: Grundlagen für eine gemeinsame Strategie zur Umsetzung der WRRL in Europa. In: Rumm, P., von Keitz, S. and Schmalholz, M. (Ed.): Handbuch der EU-Wasserrahmenrichtlinie. Inhalte, Neuerungen und Anregungen für die nationale Umsetzung, 2. edition, Berlin, 11-26, 2006.

Comiti, F., Andreoli, A., Mao, L., Lenzi, and M. A.: Wood storage in three mountain streams of the Southern Andes and its hydro-morphological effects, Earth Surface Processes and Landforms 33 (2), 244-262, https://doi.org/10.1002/esp.1541, 2008.

Comiti, F., Cadol, D., and Wohl, E. E.: Flow regimes, bed morphology, and flow resistance in self-formed step-pool channels. Water Resources Research 45 (34), W04424, 1-18, https://doi.org/10.1029/2008WR007259, 2009.

Chow, V. T.: Open-channel hydraulics, Tokyo, 1959.

Curran, J. H. and Wohl, E. E.: Large woody debris and flow resistance in step-pool channels, Cascade Ranges, Washington, Geomorphology 51 (1-3), 141-157, https://doi.org/10.1016/S0169-555X(02)00333-1, 2003.

Daniels, M. D. and Rhoads, B. L.: Effect of large woody debris configuration on three-dimensional flow structure in two low-energy meander bends at varying stages. Water Resources Research 40 (11), W11302, 1-14, https://doi.org/10.1029/2004WR003181, 2004.

Daniels, M. D. and Rhoads, B. L.: Influence of experimental removal of large woody debris on spatial patterns of three-dimensional flow in a meander bend, Earth Surface Processes and Landforms 32 (3), 460-474, https://doi.org/10.1002/esp.1419, 2007.

Davidson, S. L. and Eaton, B. C.: Modeling channel morphodynamic response to variations in large wood: Implications for stream rehabilitation in degraded watersheds, Geomorphology 202, 59-73, https://doi.org/10.1016/j.geomorph.2012.10.005, 2013.

De Cicco, P. N., Paris, E., Ruiz-Villanueva, V., Solari, L., Stoffel, M.: In-channel wood-related hazards at bridges: A review, River Research and Applications 34 (7), 617-628, https://doi.org/10.1002/rra.3300, 2018.

Dudley, S. J., Fischenich, J. C., and Abt, S. R.: Effect of woody debris entrapment on flow resistance, Journal of the American Water Resources Association 34 (5), 1189-1197, https://doi.org/10.1111/j.1752-1688.1998.tb04164.x, 1998.

Faber, R., Fuchs, M, and Puchner, G.: Numerische Simulation von Hochwässern: Von 1D zu 3D aus Anwendersicht im Ingenieurbereich, Österreichische Wasser- und Abfallwirtschaft 64 (5-6), 307-313, https://doi.org/10.1007/s00506-012-0404-0, 2012.

GeoSN – Saxon State Office of Geoinformation and Surveying (Ed.): Digital elevation model ATKIS-DGM2, 2008.

Gregory, K. J., Gurnell, A. M., and Hill, C. T.: The permanence of debris dams related to river channel processes, Hydrological Sciences Journal 30 (3), 371-381, https://doi.org/10.1080/02626668509491000, 1985.

Gurnell, A. M., Piégay, H., Swanson, F. J., and Greogry, S. V.: Large wood and fluvial processes, Freshwater Biology 47 (4), 601-619, https://doi.org/10.1046/j.1365-2427.2002.00916.x, 2002.

Hafs, A. W., Harrison, L. R., Utz, R. M., and Dunne, T.: Quantifying the role of woody debris in providing bioenergetically favorable habitat for juvenile salmon, Ecological Modelling 285, 30-38, https://doi.org/10.1016/j.ecolmodel.2014.04.015, 2014.

He, Z., Wu, W., and Shields, F. D.: Numerical analysis of effects of large wood structures on channel morphology and fish habitat suitability in a southern US sandy creek, Ecohydrology 2 (3), 370-380, https://doi.org/10.1002/eco.60, 2009.

Kail, J. and Gerhard, M. (2003): Totholz in Fließgewässern – Eine Begriffsbestimmung, Wood in streams – a definition of terms, Wasser & Boden 55 (1-2), 49-55, 2003.

Kail, J. and Hering, D.: Using large wood to restore streams in Central Europe: Potential use and likely effects, Landscape Ecology 20 (6), 755-772, https://doi.org/10.1007/s10980-005-1437-6, 2005.

Kail, J., Hering, D., Muhar, S., Gerhard, M., and Preis, S.: The use of large wood in stream restoration: Experiences from 50 projects in Germany and Austria, Journal of Applied Ecology 44 (6), 1145-1155, https://doi.org/10.1111/j.1365-2664.2007.01401.x, 2007

Keys, T. A., Govenor, H., Jones, C. N., Hession, W. C., Hester, E. T., and Scott, D. T.: Effects of large wood on floodplain connectivity in a headwater Mid-Atlantic stream, Ecological Engineering 118, 134-142, https://doi.org/10.1016/j.ecoleng.2018.05.007, 2018.

Korn, N., Jessel, B., Hasch, B., and Mühlinghaus, R.: Flussauen und Wasserrahmenrichtlinie. Bedeutung der Flussauen für die Umsetzung der Wasserrahmenrichtlinie – Handlungsempfehlungen für Naturschutz und Wasserwirtschaft, Naturschutz und Biologische Vielfalt 27, 2005.

Kramer, N. and Wohl, E. E.: Rules of the road: A qualitative and quantitative synthesis of large wood transport through drainage networks, Geomorphology 279, 74-97, https://doi.org/10.1016/j.geomorph.2016.08.026, 2017.

Lai, Y. G. and Bandrowski, D. J.: Large wood flow hydraulics: A 3d modelling approach, in: Ames, D. P., Quinn, N. W. T., Rizzoli, A. E. (Ed.): 7th International Congress on Environmental Modelling and Software in San Diego, CA, USA, 2163-2171, 2014.

Lange, C., Schneider, M., Mutz, M., Haustein, M., Halle, M., Seidel, M., Sieker, H., Wolter, C., and Hinkelmann, R.: Model-based design for restoration of a small urban river, Journal of Hydro-environment Research 9 (2), 226-236, https://doi.org/10.1016/j.jher.2015.04.003, 2015.

LfULG – Saxon State Office for Environment, Agriculture and Geology (Ed.): Zöblitz gauging station: Daily discharges 2015 and multi-annual statisitics, period 1937-2015, https://www.umwelt.sachsen.de/umwelt/wasser/download/568400_Q2015.pdf, last accessed on 24.02.2018, 2017a.

LfULG – Saxon State Office for Environment, Agriculture and Geology (Ed.): Zöblitz gauging station: Daily discharges 2008 and multi-annual statisitics, period 1937-2008, https://www.umwelt.sachsen.de/umwelt/wasser/download/568400_Q2008.pdf, last accessed on 24.02.2018, 2017b.

LVA – Saxon State Office for Surveying (Ed.): Official German topographic map, scale 1:25,000, sheet 5345, 3. edition, Dresden, 2002.

MacFarlane, W. A. and Wohl, E. E.: Influence of step composition on step geometry and flow resistance in step-pool streams of the Washington Cascades, Water Resources Research 39 (2), 1037, 1-13, https://doi.org/10.1029/2001WR001238, 2003.

Manners, R. B., Doyle, M. W., and Small, M. J.: Structure and hydraulics of natural woody debris jams, Water Resources Research 43 (6), W06432, 1-17, https://doi.org/10.1029/2006WR004910, 2007.

Moriasi, D. N., Arnold, J. G., Van Liew, M. W., Bingner, R. L., Harmel, R. D., and Veith, T. L.: Model evaluation guidelines for systematic quantification of accuracy in watershed simulations, Transactions of the American Society of Agricultural and Biological Engineers 50 (3), 885-900, https://doi.org/10.13031/2013.23153, 2007.

Nujić, M.: HYDRO_AS-2D, Ein zweidimensionales Strömungsmodell für die wasserwirtschaftliche Praxis, Benutzerhandbuch, 2006.

Pander, J. and Geist, J.: Ecological indicators for stream restoration success, Ecological Indicators 30, 106-118, https://doi.org/10.1016/j.ecolind.2013.01.039, 2013.

Petrow, T., Merz, B., Lindenschmidt, K.-E., and Thieken, A. H.: Aspects of seasonality and flood generating circulation patterns in a mountainous catchment in south-eastern Germany, Hydrology and Earth System Sciences 11, 1455-1468, https://doi.org/10.5194/hess-11-1455-2007, 2007.

Pilotto, F., Bertoncin, A., Harvey, G. L., Wharton, G., and Pusch, M. T.: Diversification of stream invertebrate communities by large wood, Freshwater Biology 59 (12), 2571-2583, https://doi.org/10.1111/fwb.12454, 2014.

R Core Team: R: A language and environment for statistical computing, R Foundation for Statistical Computing, Vienna, Austria. ISBN 3-900051-07-0, http://www.R-project.org. 2017.

Reinhardt-Imjela, C., Imjela, R., Bölscher, J., and Schulte, A.: The impact of late medieval deforestation and 20th century forest decline on extreme flood magnitudes in the Ore Mountains (Southeastern Germany), Quaternary International 475, 42-53, https://doi.org/10.1016/j.quaint.2017.12.010, 2018.

Roni, P., Beechie, T., Pess, G., and Hanson, K.: Wood placement in river restoration: Fact, fiction, and future direction, Canadian Journal of Fisheries and Aquatic Sciences 72 (3), 466-478, https://doi.org/10.1139/cjfas-2014-0344, 2015.

Ruiz-Villanueva, V., Piégay, H., Gurnell, A. M., Marston, R. A., and Stoffel, M.: Recent advances quantifying large wood dynamics in river basins: New methods and remaining challenges, Reviews of Geophysics 54 (3), https://doi.org/10.1002/2015RG000514, 2016.

Schmocker, L., and Hager, W.H.: Probability of drift blockage at bridge decks, Journal of Hydraulic Engineering 137 (4), 470-479, https://doi.org/10.1061/(ASCE)HY.1943-7900.0000319, 2011.

Seidel, M. and Mutz, M.: Hydromorphologische Entwicklung von Tieflandbächen durch Holzeinsatz – Vergleich von Einbauvarianten im Ruhlander Schwarzwasser, Hydrologie und Wasserbewirtschaftung 56 (3), 126-134, https://doi.org/10.5675/HyWa_2012,3_3, 2012.

Shields, F. D. and Gippel, C. J.: Prediction of effects of woody debris removal on flow resistance, Journal of Hydraulic Engineering 121 (4), 341-354, https://doi.org/10.1061/(ASCE)0733-9429(1995)121:4(341), 1995.

Shields, F. D. and Smith, R. H.: Effects of large woody debris removal on physical characteristics of a sand-bed river, Aquatic Conservation: Marine and Freshwater Environments 2 (2), 145-163, https://doi.org/10.1002/aqc.3270020203, 1992.

Shields, F. D., Coulton, K. G., and Nepf, H.: Representation of vegetation in two-dimensional hydrodynamic models, Journal of Hydraulic Engineering 143 (8), 02517002, 1-9, https://doi.org/10.1061/(ASCE)HY.1943-7900.0001320, 2017.

Smith, D. L., Allen, J. B., Eslinger, O., Valeciano, M., Nestler, J., and Goodwin, R. A.: Hydraulic modeling of large roughness elements with computational fluid dynamics for improved realism in stream restoration planning, in: Simon, A., Bennett, S. J., Castro, J. M. (Ed.): Stream restoration in dynamic fluvial systems: Scientific approaches, anaylses, and tools, Geophysical Monograph Series 194, 115-122, https://doi.org/10.1029/2010GM000988, 2011.

Thomas, H. and Nisbet, T.: Modelling the hydraulic impact of reintroducing large woody debris into watercourses, Journal of Flood Risk Management 5 (2), 164-174, https://doi.org/10.1111/j.1753-318X.2012.01137.x, 2012.

Wenzel, R., Reinhardt-Imjela, C., Schulte, A., and Bölscher, J.: The potential of in-channel large woody debris in transforming discharge hydrographs in headwater areas (Ore Mountains, southeastern Germany), Ecological Engineering 71, 1-9, https://doi.org/10.1016/j.ecoleng.2014.07.004, 2014.

Wilcox, A. C., Nelson, J. M., and Wohl, E. E.: Flow resistance dynamics in step-pool channels: 2. partitioning between grain, spill, and woody debris resistance, Water Resources Research 42 (5), W05419, 1-14, https://doi.org/10.1029/2005WR004278, 2006.

Wilcox, A. C. and Wohl, E. E.: Flow resistance dynamics in step-pool channels: 1. Large woody debris and controls on total resistance, Water Resources Research 42 (5), W05418, 1-16, https://doi.org/10.1029/2005WR004277, 2006.

Wilcox, A. C., Wohl, E. E., Comiti, F., and Mao, L.: Hydraulics, morphology, and energy dissipation in an alpine step-pool channel, Water Resources Research 47 (7), W07514, 1-17, https://doi.org/10.1029/2010WR010192, 2011.

Wohl, E.: Of wood and rivers: bridging the perception gap, WIREs Water 2 (3), 167-176, https://doi.org/10.1002/wat2.1076, 2015.

Wohl, E.: Bridging the gaps: An overview of wood across time and space in diverse rivers, Geomorphology 279, 3-26, https://doi.org/10.1016/j.geomorph.2016.04.014, 2017.

Wohl, E., Cenderelli, D. A., Dwire, K. A., Ryan-Burkett, S. E., Young, M. K., and Fausch, K. D.: Large in-stream wood studies: A call for common metrics, Earth Surface Processes and Landforms 35, 618-625, https://doi.org/10.1002/esp.1966, 2010.

Xu, Y. and Liu, X.: Effects of different in-stream structure representations in computational fluid dynamics models – Taking engineered log jams (EJL) as an example, Water 9 (2), 110, 1-21, https://doi.org/10.3390/w9020110, 2017.

Yen, B. C.: Open channel flow resistance, Journal of Hydraulic Engineering 128 (1), 20-39, https://doi.org/10.1061/(ASCE)0733-9429(2002)128:1(20), 2002.

Young, W. J.: Flume study of the hydraulic effects of large woody debris in lowland rivers, Regulated Rivers: Research & Management 6 (3), 203-211, https://doi.org/10.1002/rrr.3450060305, 1991.

Zambrano-Bigiarini, M.: R-package "hydroGOF", version 0.3-10, https://cran.r-project.org/web/packages/hydroGOF/hydroGOF.pdf, last accessed on 24.02.2018, 2017.

Hydrol. Earth Syst. Sci. Discuss., https://doi.org/10.5194/hess-2019-35
Manuscript under review for journal Hydrol. Earth Syst. Sci.
Discussion started: 4 February 2019

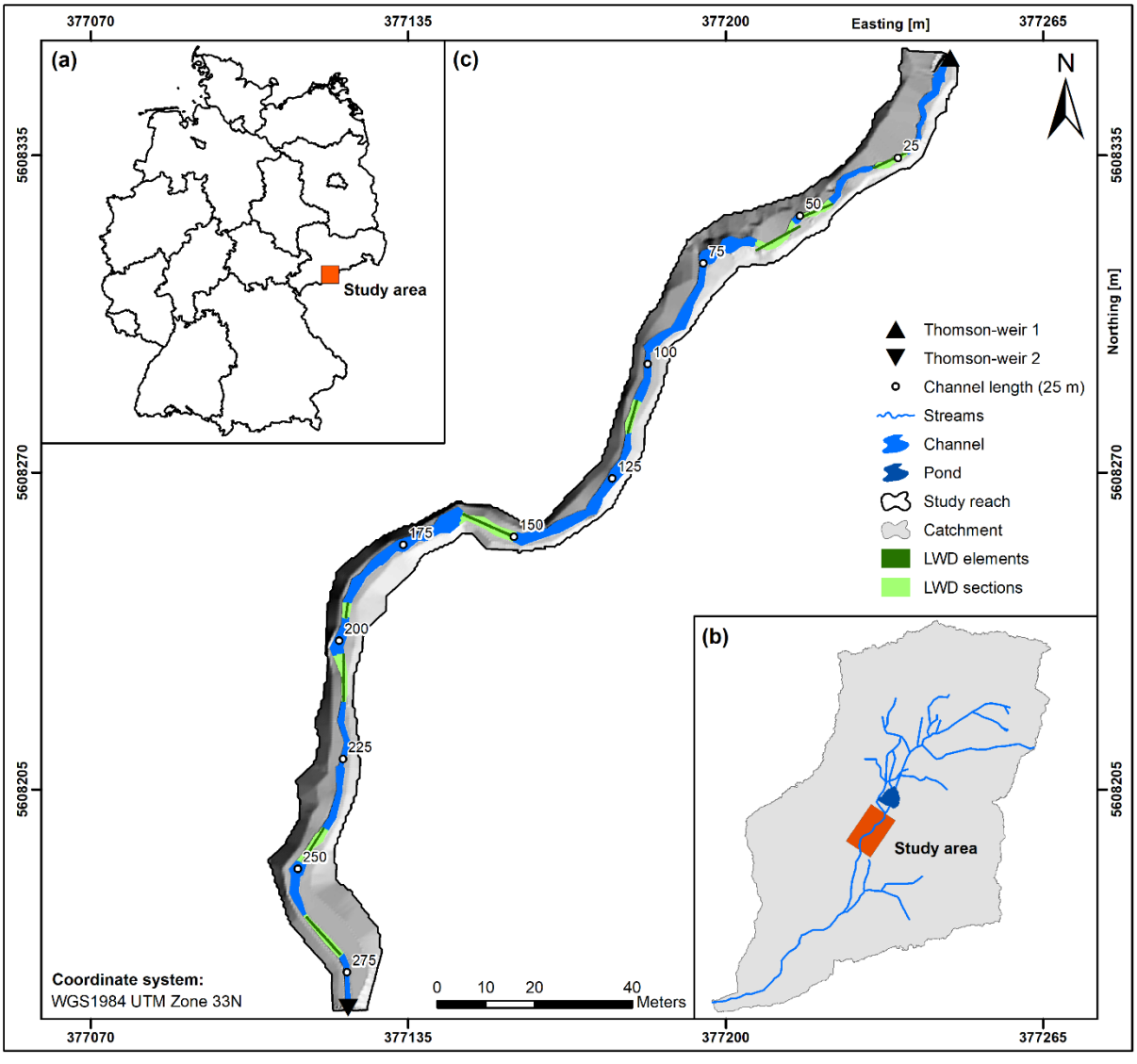

Figure 1: (a) Location of the study area in Germany (administrative units: BKG, 2018) and (b) position of the study reach in the catchment of the Ullersdorfer Teichbächel (stream network: LVA, 2002). (c) LWD affected sections and positions of discrete LWD elements in the study reach.

Hydrol. Earth Syst. Sci. Discuss., https://doi.org/10.5194/hess-2019-35
Manuscript under review for journal Hydrol. Earth Syst. Sci.
Discussion started: 4 February 2019

Hydrology and Earth System Sciences
Discussions

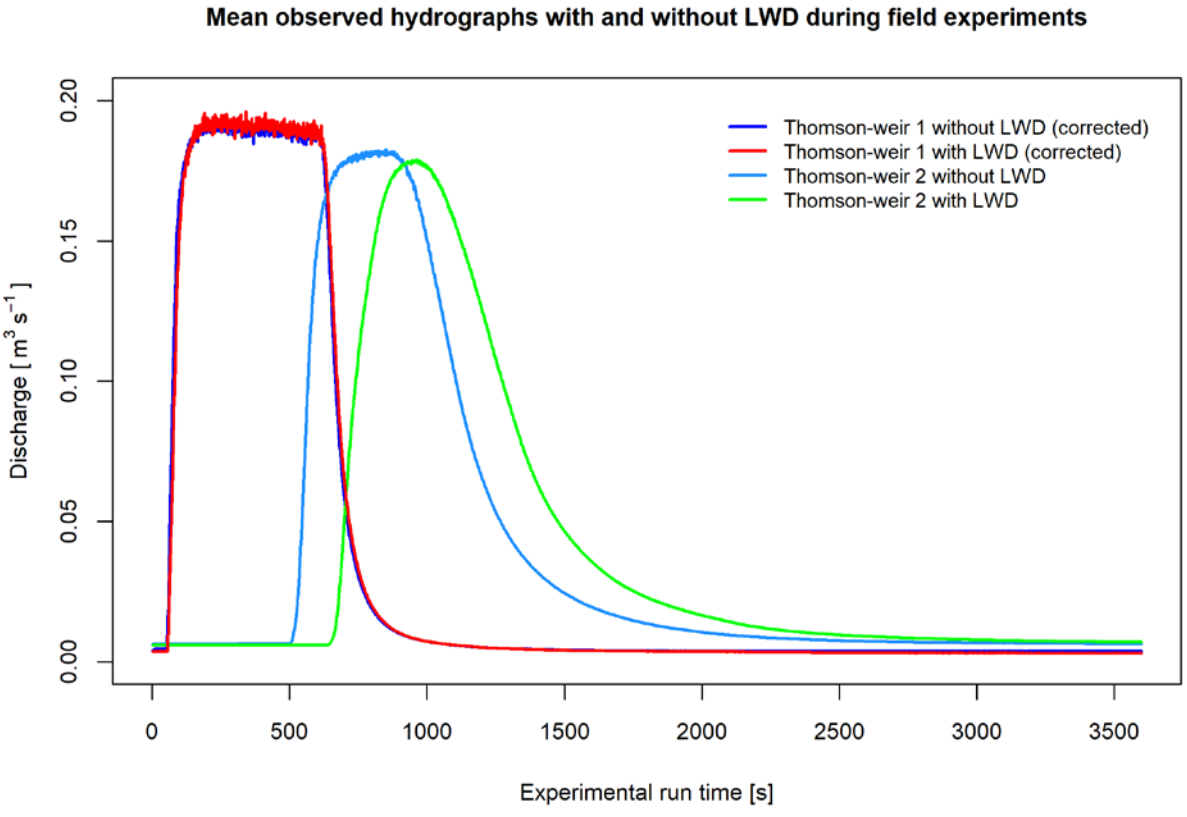

Figure 2: Average measured and corrected flood hydrographs observed during field experiments with and without stable in-channel large woody debris at both Thomson-weirs (after Wenzel et al., 2014).

Hydrol. Earth Syst. Sci. Discuss., https://doi.org/10.5194/hess-2019-35
Manuscript under review for journal Hydrol. Earth Syst. Sci.
Discussion started: 4 February 2019

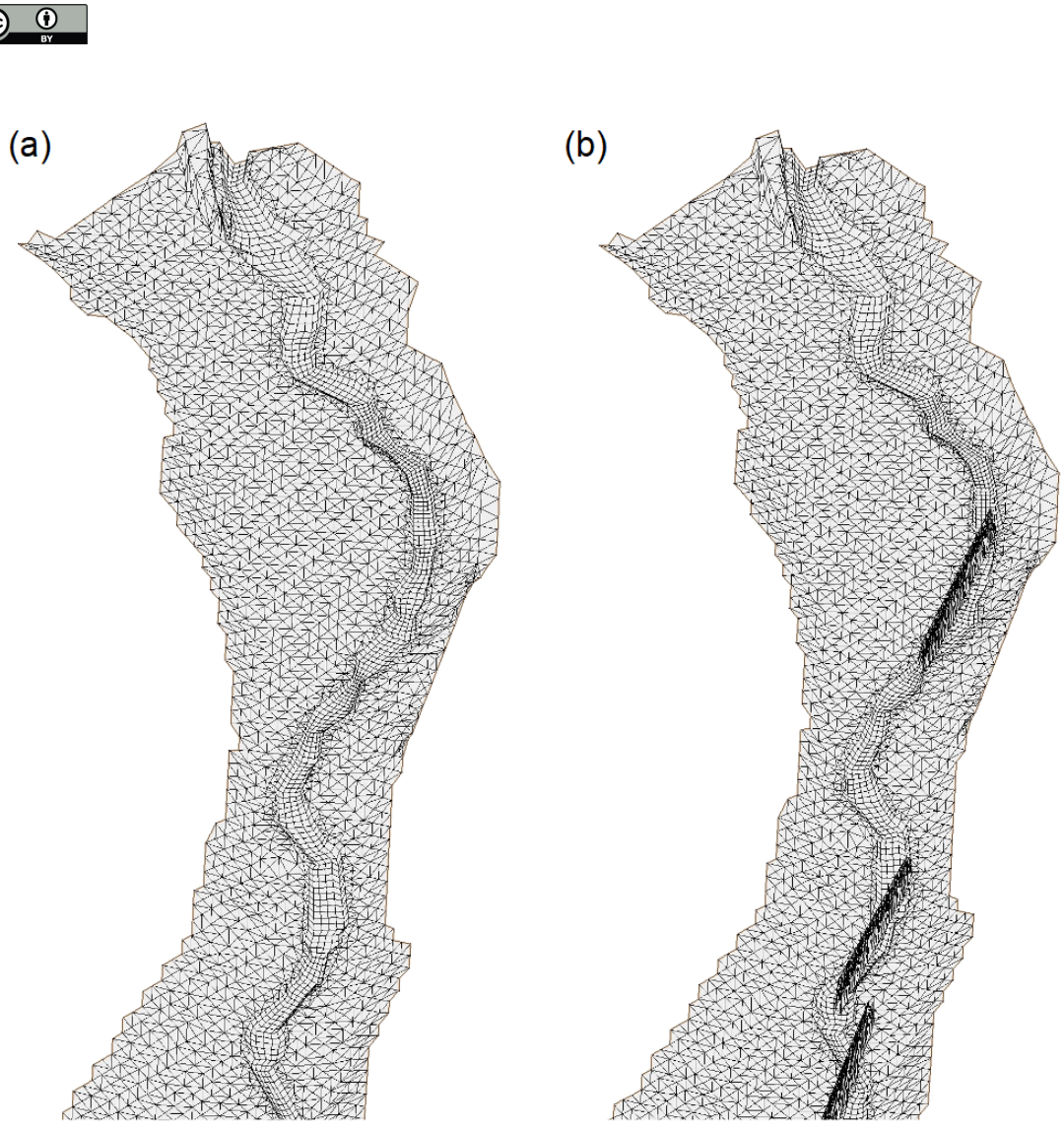

Figure 3: (a) Calculation mesh of the hydrodynamic model used in simulation variants BV, V1 and V2 with the use of variable Strickler coefficients adjusted for the entire channel (V1) or adjusted at the positions of all LWD elements only (V2) and (b) mesh with discrete LWD elements used in variant V3. Example of the first 60 m of the study reach.

Hydrol. Earth Syst. Sci. Discuss., https://doi.org/10.5194/hess-2019-35
Manuscript under review for journal Hydrol. Earth Syst. Sci.
Discussion started: 4 February 2019

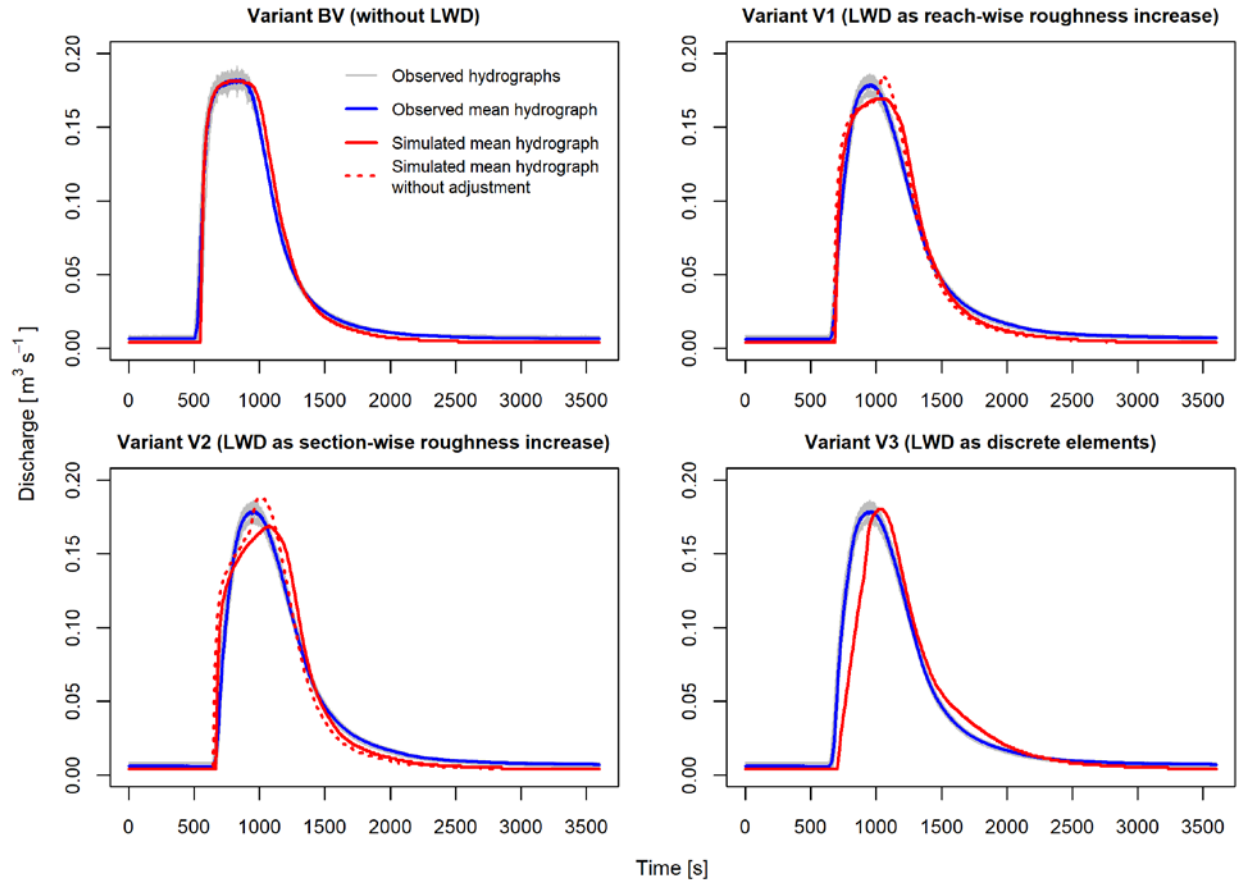

Figure 4: Best simulated mean flood hydrographs of all simulations variants with and without LWD at Thomson-weir 2. In variant V1 and V2 the best fit with and without subsequent adjustment of riparian Strickler coefficients is displayed.

Hydrol. Earth Syst. Sci. Discuss., https://doi.org/10.5194/hess-2019-35
Manuscript under review for journal Hydrol. Earth Syst. Sci.
Discussion started: 4 February 2019

Hydrology and Earth System Sciences
Discussions

Table 1: Average observed and simulated discharge sums ($m^3 h^{-1}$) at both Thomson-weirs for all simulation variants. For variant V1 and V2 discharge sums with subsequent adjustment of riparian Strickler coefficients are displayed.

Discharge sums (3600 s) for each variant ($m^3 h^{-1}$)	Base-Variant	Variant 1	Variant 2	Variant 3
Thomson-weir 1 (observed, corrected)	128	128	128	128
Thomson- weir 2 (observed)	132	133	133	133
Thomson-weir 1 (simulated)	128	128	128	128
Thomson-weir 2 (simulated)	128	128	128	123
Difference between observed and simulated values (Thomson-weir 2)	-4	-5	-5	-10
Observed difference between Thomson-weir 1 and 2	-4	-5	-5	-5

Table 2: Calculated statistical goodness-of-fit parameters for all simulation variants. For variant V1 and V2 goodness-of-fit parameters with and without subsequent adjustment of riparian Strickler coefficients are displayed.

Goodness-of-fit parameters	Basie-Variant	Variant 1 without adjustment	Variant 1	Variant 2 without adjustment	Variant 2	Variant 3
NSE	0,99	0,97	0,98	0,94	0,96	0,90
RSR	0,11	0,18	0,14	0,24	0,19	0,32
PBIAS (%)	- 3,5	- 3,6	- 3,7	- 4,2	- 4,0	- 7,7